NASA TECHNICAL NOTE

NASA TN D-5429

HEAT-TRANSFER CHARACTERISTICS OF A WATER-TO-CRYOGENIC-HYDROGEN HEAT EXCHANGER

by Walter F. Weiland, Jr., and Donald W. Adams

Lewis Research Center
Cleveland, Ohio

NATIONAL AERONAUTICS AND SPACE ADMINISTRATION • WASHINGTON, D. C. • SEPTEMBER 1969

1. Report No. NASA TN D-5429	2. Government Accession No.	3. Recipient's Catalog No.
4. Title and Subtitle HEAT-TRANSFER CHARACTERISTICS OF A WATER-TO-CRYOGENIC-HYDROGEN HEAT EXCHANGER		5. Report Date September 1969 6. Performing Organization Code
7. Author(s) Walter F. Weiland, Jr., and Donald W. Adams		8. Performing Organization Report No. E-4937
9. Performing Organization Name and Address Lewis Research Center National Aeronautics and Space Administration Cleveland, Ohio 44135		10. Work Unit No. 120-27-04-54-22 11. Contract or Grant No.
12. Sponsoring Agency Name and Address National Aeronautics and Space Administration Washington, D.C. 20546		13. Type of Report and Period Covered Technical Note 14. Sponsoring Agency Code

15. Supplementary Notes

16. Abstract

Heat-transfer and pressure drop measurements were obtained for a heat exchanger suitable for regeneratively cooling the water in a water-moderated nuclear rocket reactor. The heat exchanger was of shell-and-tube design having parallel fluid flow with cryogenic hydrogen inside the tubes. The ranges of conditions investigated for steady-state operation are inlet water temperature from 600° to 660° R (333 to 367 K), inlet hydrogen temperature from 100° to 180° R (55.6 to 100 K), inlet fluid pressure of approximately 700 psia (483×10^4 N/m^2), and flow in the turbulent region. The investigation included conditions where ice is expected to be formed on the tubes. The results are compared with predicted values. The transient conditions investigated simulated expected conditions during reactor startup.

17. Key Words (Suggested by Author(s)) Heat transfer Heat exchanger	18. Distribution Statement Unclassified - unlimited		
19. Security Classif. (of this report) Unclassified	20. Security Classif. (of this page) Unclassified	21. No. of Pages 32	22. Price * $3.00

*For sale by the Clearinghouse for Federal Scientific and Technical Information
Springfield, Virginia 22151

HEAT-TRANSFER CHARACTERISTICS OF A WATER-TO-CRYOGENIC-HYDROGEN HEAT EXCHANGER

by Walter F. Weiland, Jr., and Donald W. Adams

Lewis Research Center

SUMMARY

The overall heat-transfer coefficient and fluid pressure drops were measured for a shell-and-tube heat exchanger suitable for regeneratively cooling the water in a water-moderated nuclear reactor. The fluid flow is parallel. Cryogenic hydrogen flowed inside the tubes, and water inside the shell.

Measurements were obtained during steady state and transient operation. The ranges of conditions investigated for steady-state operation were inlet hydrogen temperature from 100° to 180° R (55.6 to 100 K), inlet water temperature from 600° to 660° R (333 to 367 K), water and hydrogen inlet pressure of approximately 700 psia (483×10^4 N/m^2), and fluid flow in the turbulent region. The transient conditions investigated were similar to what might be expected during reactor startup.

The results of the investigation showed that

1. Steady-state operation can be attained for conditions where freezing exists.

2. At constant water flow rate and constant fluid inlet temperatures the overall heat-transfer coefficient increases with increasing hydrogen flow rate in the non-ice region. Once ice forms, the overall coefficient remains essentially constant with increasing hydrogen flow rate.

3. For the transient conditions investigated the overall heat-transfer coefficient can be reasonably well represented by the steady-state value measured at the corresponding fluid conditions.

The measured overall heat-transfer coefficient is compared with values calculated assuming uniform mass velocity distribution, no heat lost to the surroundings, no heat conducted axially along the tubes or shell, smooth passages, and fully developed turbulent flow. The measured overall heat-transfer coefficients for the non-ice region are generally within ±10 percent of the predicted values. In the ice region the measured values are 15 to 35 percent above the predicted overall coefficients.

INTRODUCTION

Heat exchangers that utilize a coolant at a temperature below the freezing point of the liquid being cooled are of interest in some space vehicle systems. One application of such a heat exchanger is for regeneratively cooling the moderator water in a water-moderated nuclear rocket reactor. Here the cryogenic propellant is used as the coolant. Other applications may be found in space vehicle systems where a cryogen is readily available as a coolant.

One potential problem encountered in the operation of such a heat exchanger is solidification of the liquid on the cold surface. This problem would most likely occur at low liquid flow rates and low fluid temperatures. Under extreme conditions the frozen layer may become thick enough to completely block the flow passage. Even though blockage does not occur, the presence of a frozen liquid layer will affect the heat-transfer characteristic of the heat exchanger. In addition, some question arises as to whether steady-state conditions can be attained under freezing conditions.

To design a heat exchanger for operation over a range of conditions that includes freezing, it is necessary to determine the conditions at which freezing occurs and the thickness of the frozen layer. This requires a knowledge of the liquid-frozen layer interface temperature and the contact thermal resistance between the frozen layer and the wall.

A literature search revealed two investigations (refs. 1 and 2) that appear to be most applicable to the present investigation and are discussed herein. A more complete literature survey of the freezing process is contained in reference 1.

An analysis and experimental study of the transient freezing process in a flowing liquid is reported in reference 1. The study was conducted using water flowing over a plate chilled by a cold flowing fluid. It was found that for steady-state conditions the water-ice interface temperature was within a fraction of a degree of the equilibrium freezing temperature. It was also shown that the thermal contact resistance between the ice and the wall was small.

An experimental study of a single concentric tube, counterflow, heat exchanger is reported in reference 2. Here cryogenic nitrogen or hydrogen flowed through the inner tube and water through the outer tube. The tests were conducted with the exchanger in a horizontal position. The Reynolds numbers were in the turbulent range. It was shown that the heat exchanger could be operated under steady-state conditions with an ice layer present.

References 1 and 2 are investigations of single flow passages where the mass velocities are well defined. A multitube heat exchanger may be designed assuming uniform mass velocities for each tube. However, in reality, this may not be the case. Nonuniform mass velocities as well as local disturbances such as tube spacers will result in variations of the heat-transfer coefficient from tube to tube. These variations may have a negligible effect on the performance of the heat exchanger when no frozen layer exists.

But in the presence of a frozen layer these variations may greatly affect exchanger performance because the layer thickness is dependent on the fluid heat-transfer coefficient. Therefore, calculations performed assuming a single flow passage or uniform mass velocity distribution may not be applicable to a multitube heat exchanger at or near freezing conditions.

A multitube heat exchanger that will operate at conditions which may include a freezing situation is proposed for regeneratively cooling the moderator in a water-moderated nuclear rocket reactor. Such an exchanger must operate effectively for steady-state conditions as well as during startup of the reactor. Although the exchanger would not normally operate under a freezing situation, off design conditions or a variation in the expected startup conditions may result in a freezing situation. Therefore, an investigation was initiated at the NASA Lewis Research Center to determine the heat-transfer characteristics of such a heat exchanger. The tests were conducted at the Plum Brook Station.

The heat exchanger investigated herein is of shell-and-tube design and is composed of 19 tubes arranged in a triangular array. Cryogenic hydrogen flowed inside the tubes and water in the shell. The flow was parallel.

Heat-transfer and pressure drop data were obtained for steady-state as well as transient conditions. The steady-state conditions were expected to include both nonfreezing and freezing situations. For steady-state conditions data were taken over the following range of conditions: hydrogen inlet temperature from 100° to 180° R (55.6 to 100 K), inlet water temperature from 600° to 660° R (333 to 367 K), inlet water and hydrogen pressure of approximately 700 psia (483×10^4 N/m^2), and flow in the turbulent region. The transient conditions investigated were similar to what might be expected during reactor startup. The results are compared with predicted values. The calculations were made assuming uniform mass velocity distribution, no heat lost to the surroundings, no heat conducted axially along the tubes or shell, smooth passages, and fully developed turbulent flow.

APPARATUS

Flow System

A schematic diagram of the flow system is shown in figure 1. The system consists of a separate water and hydrogen system. The desired water temperature at the inlet to the heat exchanger was obtained by mixing hot and ambient temperature water supplied from separate tanks. High pressure nitrogen gas was used to force water from the supply tanks through the system. The water from each tank flowed through a separate flow-control valve after which the two streams were mixed at a tee. The temperature

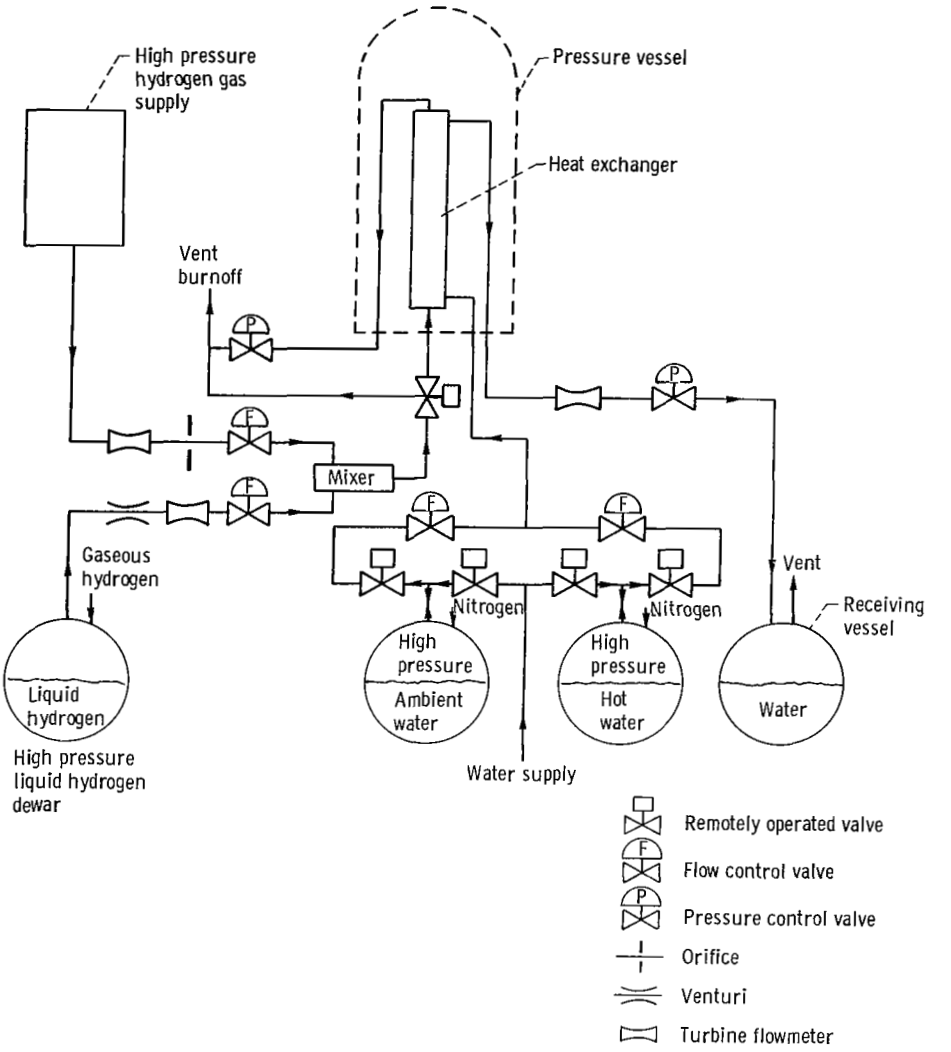

Figure 1. - Flow schematic.

of the mixture at this point was used to automatically adjust the flow-control valves to obtain the desired temperature at the inlet of the heat exchanger. These valves were also used to obtain the desired water flow rate. The water then flowed through the test section, a turbine type flowmeter, a pressure regulating valve, and into a receiving tank at atmospheric pressure. Deionized water was used for the tests.

Liquid and gaseous hydrogen were mixed to obtain the desired hydrogen temperature at the inlet to the heat exchanger. The gas was supplied from high pressure trailers. The gaseous hydrogen flowed from the trailers through a turbine flowmeter, an orifice, and a flow-control valve and into a mixing chamber. Liquid hydrogen was forced through the system by pressurizing a dewar with gaseous hydrogen. From the dewar the liquid hydrogen flowed through a venturi, a turbine flowmeter, a flow-control valve, and into

the mixing chamber. The two flow-control valves, as in the water system, could be operated independently to control the temperature of the mixture or together to control the total hydrogen flow rate. From the mixing chamber the hydrogen passed through a three-way valve, the heat exchanger, a pressure-control valve, and into the exhaust where it was burned. The three-way valve located near the inlet to the heat exchanger was used to bypass the heat exchanger during cool-down of the piping.

Test Section

The test section is a shell-and-tube heat exchanger having 19 tubes arranged in a triangular array. The spacing, measured between tube centers, is 0.475 inch (1.21 cm). The outside diameter of the tubes is 0.375 inch (0.952 cm) and the wall thickness is 0.035 inch (0.0889 cm). The tubes are separated by spacers so arranged that the resulting reduction in flow area does not exceed 30 percent. Figure 2 shows the heat exchanger components and tube spacer arrangement. Figure 3 shows the shell dimensions and the

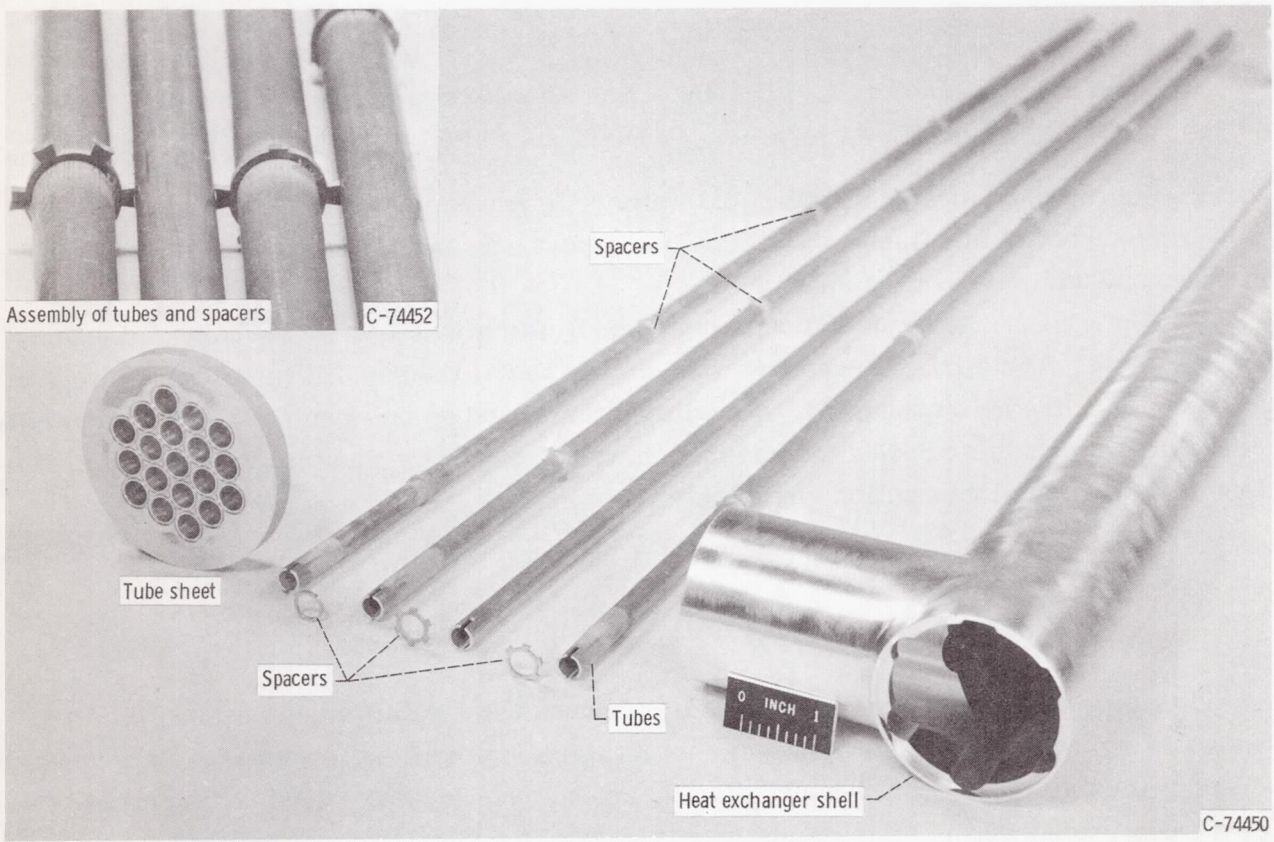

Figure 2. - Heat exchanger components.

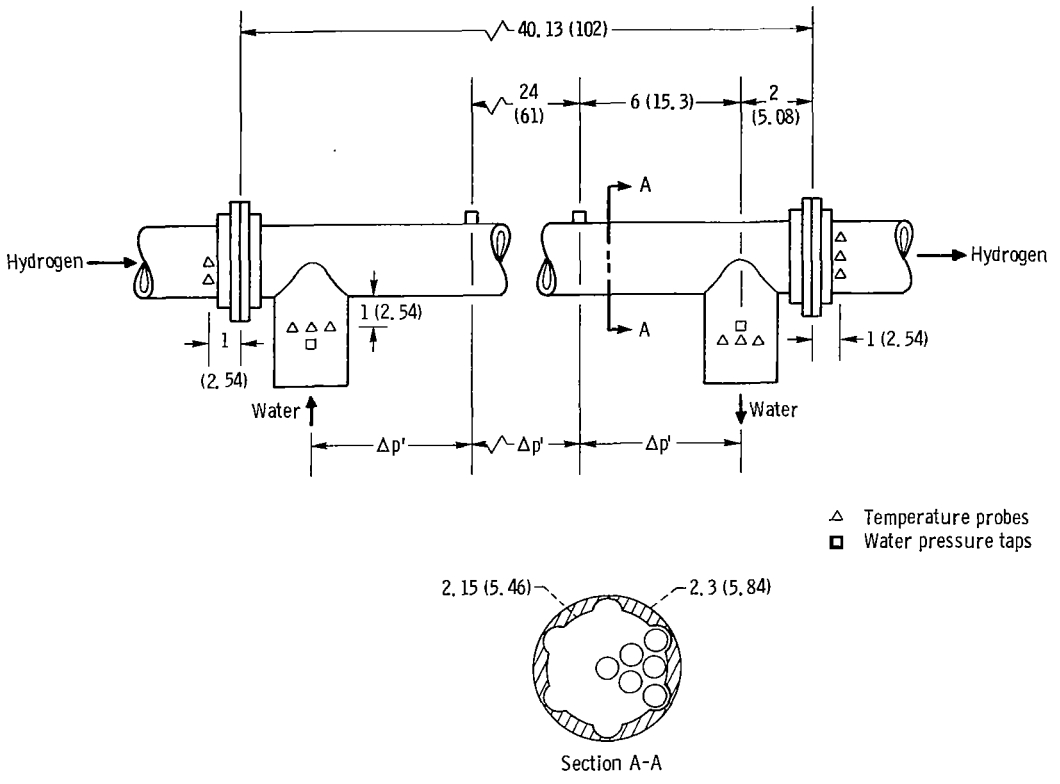

Figure 3. - Heat exchanger shell dimensions and instrumentation location. (All linear dimensions are in inches (cm).)

location of the thermocouple probes and water side pressure taps. The heat exchanger was constructed of aluminum. The flow in the heat exchanger was parallel with hydrogen in the tubes and water in the shell.

The heat exchanger was enclosed in a vessel which was pressurized with nitrogen during a run. The nitrogen pressure was maintained at the same level as the hydrogen at the inlet to the heat exchanger. Equalizing the pressure between the inside and outside of the heat exchanger allowed the use of lightweight hardware thus minimizing the heat loss due to thermal conduction along the piping.

Instrumentation

The locations of the various temperature probes and water-side pressure taps are shown in figure 3. The inlet hydrogen temperature for the first few steady-state runs was measured using three copper-constantan thermocouples located 1 inch (2.54 cm) upstream of the heat exchanger inlet and a platinum resistance probe located 2 feet (60.9 cm) further upstream. Comparison of these temperature measurements with other temperatures

throughout the hydrogen system showed that the platinum probe gave the most reliable reading at low temperatures. The temperature measured by the platinum probe was used as the inlet hydrogen temperature for these runs. For subsequent runs two of the thermocouples were replaced with platinum resistance probes. The average reading of these two probes was used as the hydrogen inlet temperature. These probes generally agreed to within 2° R (1.1 K). A maximum difference of 6° R (3.3 K) occurred for one run. Comparison of these probes with the one located 2 feet (60.9 cm) upstream showed an agreement within 6° R (3.3 K).

The outlet hydrogen temperature was taken as the average of three copper-constantan thermocouples located 1 inch (2.54 cm) downstream of the exchanger outlet. One thermocouple was located at the centerline of the pipe and two halfway from the centerline to the pipe wall. The agreement of these thermocouples for the majority of the steady-state runs ranged from 3° to 7° R (1.7 to 3.9 K) for a temperature above 200° R (111 K). A maximum difference of 11° R (6.1 K) occurred for one run. Below 200° R (111 K) the difference reached 21° R (11.7 K).

To determine whether the average of the three thermocouples resulted in a reliable mixed gas temperature, three additional thermocouples were located downstream of a 180° bend in the piping. With the exception of one run, the average of these thermocouples was within 2° R (1.1 K) of the temperature measured at the exchanger outlet. The good agreement between the two sets of thermocouples indicates that the average of the three thermocouples at the outlet of the heat exchanger was a good measure of the mixed outlet gas temperature.

The water temperature was measured 1 inch (2.54 cm) from the heat exchanger shell in the inlet pipe and in the outlet pipe. Three copper-constantan thermocouples were used at these two locations. The thermocouples at each location agreed within 3° R (1.7 K) or less.

A static pressure tap was located 0.21 inch (0.534 cm) from each end of one heat exchanger tube. These taps were used to measure the hydrogen inlet static pressure and the pressure drop across the heat exchanger.

The water inlet static pressure was measured in the inlet pipe at a location 1 inch (2.54 cm) from the heat exchanger shell. Static-pressure drops were measured at various locations along the water passage as shown in figure 3. The pressure drop in the center 2 feet (60.9 cm) of the exchanger was used for comparison with predicted values. All pressure measurements were made with pressure transducers.

The water flow rate was measured downstream of the heat exchanger with a turbine flowmeter.

The liquid and gaseous hydrogen flow rates were measured with turbine flowmeters prior to mixing. In addition, the liquid flow was measured with a venturi, and the gas flow with a sharp edge orifice. Agreement between the two methods of flow measurement

was generally better than 3 percent for both fluids. However, the agreement was not good at extremely low flow rates (near one-tenth full indicator reading).

Controls

The flow rate, inlet temperature, and inlet pressure of the hydrogen and water were automatically controlled. The desired value of each parameter with respect to time was programed into a controller prior to a run. Comparison of this value with the measured value during a run supplied the signal necessary to adjust the appropriate control valve.

The inlet temperature and flow rate of the hydrogen and water were controlled by the flow-control valves located upstream of the mixing point in each system (fig. 1). The temperature of the mixed fluid was regulated by adjusting one valve with respect to the other, but for flow control, the valves opened or closed together.

The inlet pressures of hydrogen and water were maintained at the desired levels by the pressure control valves located downstream of the heat exchanger.

Data Recording

The voltage signals from the pressure transducers, temperature sensing probes, and the turbine flowmeters were recorded on magnetic tape in a high speed digital recording system. The recording system capabilities and the number of parameters recorded made it possible to record the signal from each instrument approximately once every 1/40 of a second. The length of time over which data were recorded varied according to the test being conducted. For steady-state runs the time was generally 60 seconds while for transient runs the data were recorded during the ramp up (30, 60, or 120 sec) plus 60 seconds after the ramp ended.

PROCEDURE

Operation

Prior to the start of a run, the controller was programed for the run desired and the dewar and water tanks were filled. The tanks were pressurized and liquid hydrogen flow was started for cool-down of the piping. The three-way valve was set so that the liquid hydrogen bypassed the heat exchanger. When cool-down was completed, the hydrogen flow was stopped, and the three-way valve was opened to the heat exchanger. The water

and hydrogen flow were manually started and increased to a value large enough so that the controller operated effectively. At this point the procedure followed depended on whether the run was for transient or steady-state conditions.

For steady-state conditions the controller was engaged and the ramp started. When the controlled parameters had been ramped to the predetermined values, a "hold" was initiated manually. During a hold, the controlled parameters are maintained automatically at the values called for at the time the hold was initiated. When the system attained thermal equilibrium, the data were recorded. After the data were recorded, the hold was released, and the system was automatically returned to the initial conditions.

For transient runs the controller was engaged, and the system was allowed to reach thermal equilibrium. Once thermal equilibrium was attained, the ramp and the recorder were started. At the end of the ramp up there was an automatic 60 second hold, and the parameters were then ramped down to the initial conditions.

Data Reduction

A computer code was utilized to reduce the data on the magnetic tape. The data were reduced at various intervals of time depending on the type of run. For steady-state runs the interval was 3 seconds, and for transients the interval was 1 second. At each interval the value of the parameter was taken as the average of 24 consecutive readings. The average was taken to reduce the effect of an extraneous signal or noise that might otherwise be included in a single reading. The total run time involved for recording 24 readings of a particular parameter is approximately 0.6 second. For transient conditions the average value represents the value at the midpoint of the time interval. The average value is a good representation as the time interval is short and the ramp rate small. The maximum ramp rates were as follows: $T_1' = 3^{\circ}$ R per second (1.7 K/sec), $T_1'' = 6.5^{\circ}$ R per second (3.6 K/sec), $w' = 3$ percent of maximum flow rate, and $w'' = 3$ percent of maximum flow rate.

The overall heat-transfer coefficient was calculated from the equation

$$U = \frac{Q}{S'' \Delta T_m} \tag{1}$$

where Q is the heat transferred between the fluids, S'' is the hydrogen side heat-transfer surface area, and ΔT_m is the log mean temperature difference between the two fluids. (Symbols are defined in appendix A.)

For no heat loss to the surroundings, the heat transferred Q can be represented by either the heat released from the water or the heat absorbed by the hydrogen. The heat released from the water was calculated from the equation

$$Q' = w'c'_p(T'_1 - T'_2) \tag{2}$$

The specific heat of the water c'_p was assumed equal to 1.0.

The heat absorbed by the hydrogen was calculated from the equation

$$Q'' = w''(H''_2 - H''_1) \tag{3}$$

where H''_1 and H''_2 are the enthalpy of the hydrogen at the inlet and outlet, respectively.

The log mean temperature difference ΔT_m was calculated from the equation

$$\Delta T_m = \frac{(T'_1 - T''_1) - (T'_2 - T''_2)}{\ln \dfrac{(T'_1 - T''_1)}{(T'_2 - T''_2)}} \tag{4}$$

The properties of the hydrogen were obtained from reference 3. The flow rates of the gaseous and liquid hydrogen measured with the turbine meters were used in the calculations.

DISCUSSION OF RESULTS

Heat Balance

The heat balance for the heat exchanger can be written as

$$Q'' = Q' - Q_L$$

where Q'' is the heat absorbed by the hydrogen, Q' is the heat given up by the water, and Q_L is the heat lost to the surroundings by convection, conduction, and radiation.

The ortho-para composition of the hydrogen must be known to determine the enthalpy and hence the heat absorbed by the hydrogen (eq. (3)). Since the hydrogen supplied to the test section was obtained by mixing gaseous and liquid hydrogen, the composition and mass flow rate of both must be considered.

The composition of the liquid hydrogen was approximately 100 percent para. The gaseous hydrogen composition could vary from 100 percent para to 75 percent ortho and 25 percent para. When the trailer is filled the composition is 100 percent para. The composition will then change until equilibrium is reached (75 percent ortho - 25 percent para). The time required to reach equilibrium is long compared with the residence time

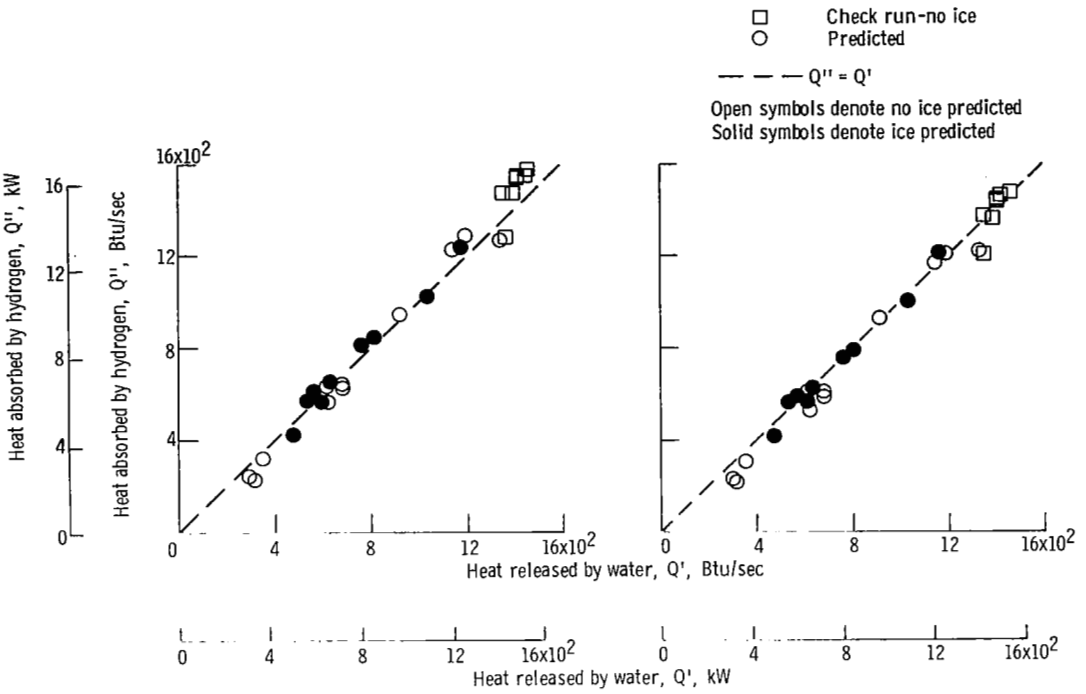

(a) Properties evaluated for para hydrogen.

(b) Properties evaluated for normal gas and para liquid hydrogen.

Figure 4. - Heat balance.

of the hydrogen in the trailer. Therefore, the ortho-para composition is most likely to be between the two extreme values.

Because the ortho-para composition was not measured during the tests, Q'' was calculated for the two extreme compositions. The resulting heat balance is shown in figure 4. Here the heat absorbed by the hydrogen is plotted as a function of the heat released by the water. Included for comparison is a dashed line which represents Q'' equal to Q'. The solid symbols represent data at fluid conditions where ice is predicted, and the open symbols where no ice is predicted. The ortho-para composition of the gaseous hydrogen is assumed to be 100 percent para in figure 4(a) and 75 percent ortho-25 percent para in figure 4(b).

It can be seen in figures 4 that a good heat balance was obtained for both methods of calculating Q''. In figure 4(a) nearly all the data are within ±10 percent of the dashed line. In figure 4(b) the heat balance is slightly better. The maximum difference in Q'' that results from the variation in the gaseous hydrogen ortho-para composition is 7 percent.

To determine the repeatability of the experimental data, the first run of each day's series of runs was taken at approximately the same fluid conditions. These data are rep-

resented by the square data symbols in figure 4. With the exception of one run the heat balance for these data are within a band represented by 5 percent of the total heat transferred. The good repeatability of the data indicates that the instrumentation or reading error is generally small. At the low fluid flow rates, as represented by $Q' = 300$ Btu per second, the flow measuring devices are at the low and hence less accurate part of their range. The repeatability is not expected to be as good for these data.

It has been shown that the heat balance without consideration of the heat lost to the surroundings Q_L is generally within ±10 percent. In addition, a large portion of the difference between the heat absorbed by the hydrogen and that released by the water can be accounted for as experimental error and the effect of the ortho-para composition. Thus, the heat loss term Q_L is expected to be small compared with the heat transferred between the fluids. Calculations verified that Q_L was small and does not exceed 1 percent of the heat released by the water. Therefore, Q_L will be neglected in the heat-transfer calculations.

The heat released by the water was used as the heat transferred Q in equation (1). The hydrogen fluid conditions (low temperature and fluid mixing), the use of two flowmeters, and the effect of the ortho-para composition presented greater possibilities of error than did the water fluid conditions.

Heat-Transfer Coefficient

The overall heat-transfer coefficient for the heat exchanger investigated herein will tend to increase with an increasing hydrogen or water flow rate and increasing fluid temperatures. However, as the hydrogen flow rate is increased the tube wall temperature is reduced. If the temperature is reduced to the freezing point of the water, ice forms on the tube wall. The thermal resistance of the ice will reduce the overall heat-transfer coefficient. Therefore, in a freezing situation an increase in the hydrogen flow rate will not necessarily result in an increase in the overall heat-transfer coefficient.

To show the variation of the overall heat-transfer coefficient with hydrogen flow rate, calculations were made using the method and equations described in appendix B. The results are shown in figure 5. The reciprocal of the overall heat-transfer coefficient (total thermal resistance) rather than the overall coefficient is plotted as it represents the sum of the thermal resistance of the water film, the ice layer, the tube wall, and the hydrogen film. The thermal resistances were calculated from the heat flux and temperatures obtained using the method and equations described in appendix B. The fluid conditions are a water flow rate of 8 pounds per second (3.63 kg/sec), an inlet hydrogen temperature of 140° R (77.8 K), and a water inlet temperature of 650° R (361 K).

Figure 5 shows that the total thermal resistance decreases with increasing hydrogen flow until ice forms. Once ice forms, the total thermal resistance remains nearly con-

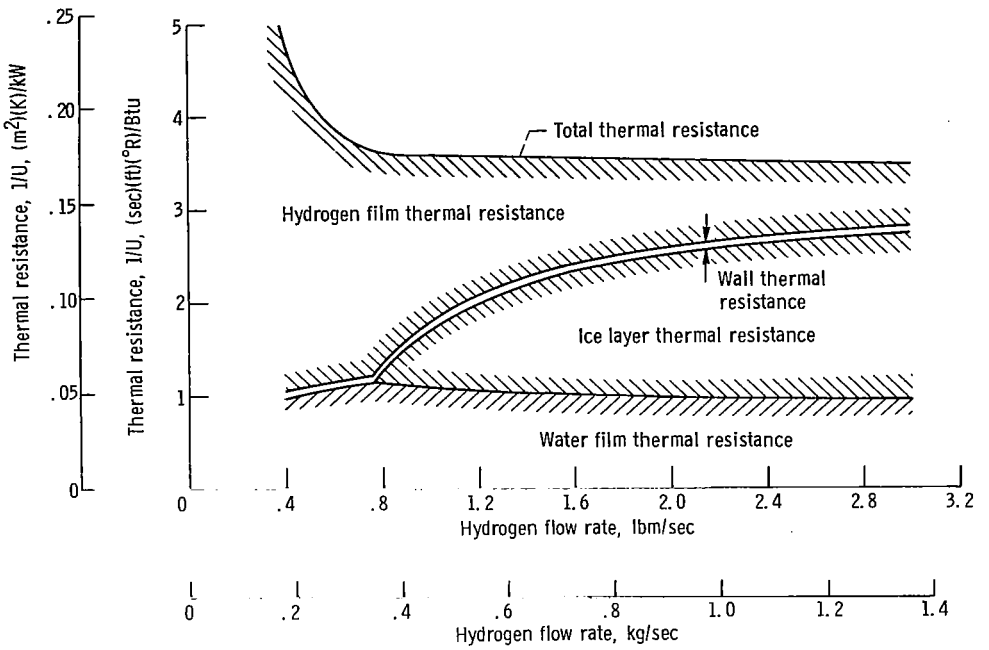

Figure 5. - Variation of thermal resistance with hydrogen flow rate. Water flow rate, 8 pounds mass per second (3.63 kg/sec); hydrogen inlet temperature, 140° R (77.8 K); water inlet temperature, 650° R (361 K).

stant with increasing hydrogen flow. The fact that the decrease in the hydrogen film resistance is nearly equal to the increase in ice layer thermal resistance may be unique to this heat exchanger design.

The small decrease in the water-side thermal resistance with an increase in the hydrogen flow is due to the increase in the mass velocity of the water (increased ice blockage) and the increase in the heat transfer surface area represented by the ice-water interface.

The variation of the overall heat-transfer coefficient over the range of conditions investigated herein is shown in figure 6. Here, the measured and predicted overall coefficients are plotted as a function of hydrogen flow rate for two water flow rates. Figure 6 shows three sets of fluid inlet temperatures. The predicted values are represented by a band enclosed by two sets of lines. The lower line represents the overall heat-transfer coefficient calculated assuming a water-side heat-transfer coefficient for fully developed flow in a smooth passage. The upper line represents the overall coefficient resulting from an increase in the water-side heat-transfer coefficient of 20 percent over that predicted in a smooth passage. Some increase in the water-side coefficient would be expected because of the increased turbulence from the tube spacers and the cross flow at the inlet and outlet of the water passage. The 20-percent increase is arbitrary. The solid lines (fig. 6) represent conditions where no ice is predicted, and the dashed lines where

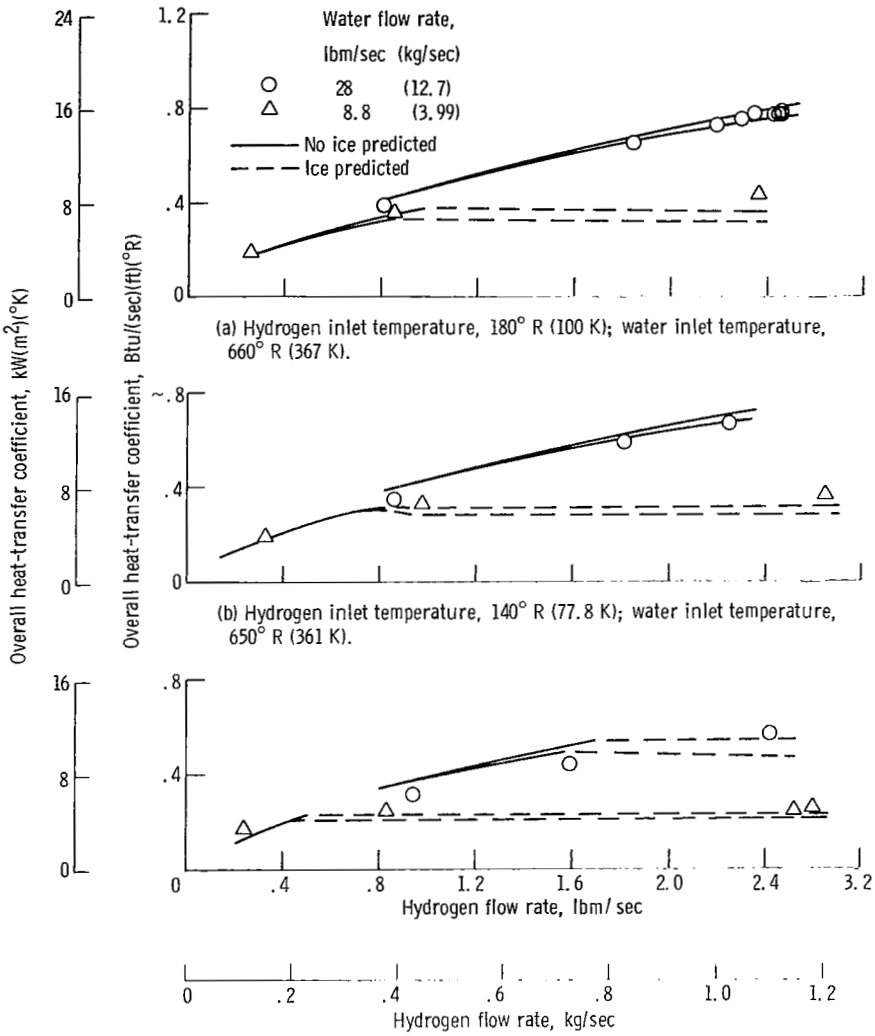

(a) Hydrogen inlet temperature, 180° R (100 K); water inlet temperature, 660° R (367 K).

(b) Hydrogen inlet temperature, 140° R (77.8 K); water inlet temperature, 650° R (361 K).

(c) Hydrogen inlet temperature, 100° R (55.6 K); water inlet temperature, 600° R (333 K).

Figure 6. - Variation of overall heat-transfer coefficient with fluid conditions.

ice is predicted. The method and equations used to obtain the predicted values are described in appendix B.

The general variation of the measured overall heat-transfer coefficient with fluid conditions is similar to that predicted. The agreement with predicted values varies over the range of fluid conditions investigated. In the non-ice region the data are in good agreement with the predicted values, being generally within ±10 percent. In the ice region the data are from 15 to 35 percent above the value predicted for heat transfer in a smooth passage (lower line in fig. 6). The agreement is improved when the predicted water-side heat-transfer coefficient is increased (upper line). This indicates that the water-side heat-transfer coefficient is somewhat greater than that predicted in a smooth passage.

One question of interest in this investigation was whether steady-state operation can be attained under a freezing situation. Steady-state operation was attained for all fluid conditions investigated including the most severe freezing conditions (high hydrogen flow rate at low water flow rate and inlet temperatures). No method was available to visually detect the existence of ice during a test. However, the reasonably good agreement between predicted and measured overall heat-transfer coefficient indicated that ice was present for most of the data in the region where ice was predicted. The conditions at which the formation of ice is questionable are those at or near the hydrogen flow rate where ice is first predicted.

Pressure Drop - Hydrogen Side

The measured pressure drop across a single tube is compared with the predicted value in figure 7. Here the measured hydrogen pressure drop is plotted as a function of the predicted hydrogen pressure drop at three sets of inlet fluid temperatures. Data below a hydrogen flow of 0.3 pound mass per second (0.136 kg/sec) are not included as the actual pressure drop is small and the instruments (flow and pressure) are at the low and hence less accurate part of their range.

When no ice is predicted, the measured pressure drop for the majority of the runs is within 20 percent of the predicted value. When ice is predicted, the majority of the data exceeds the predicted pressure drop by more than 20 percent.

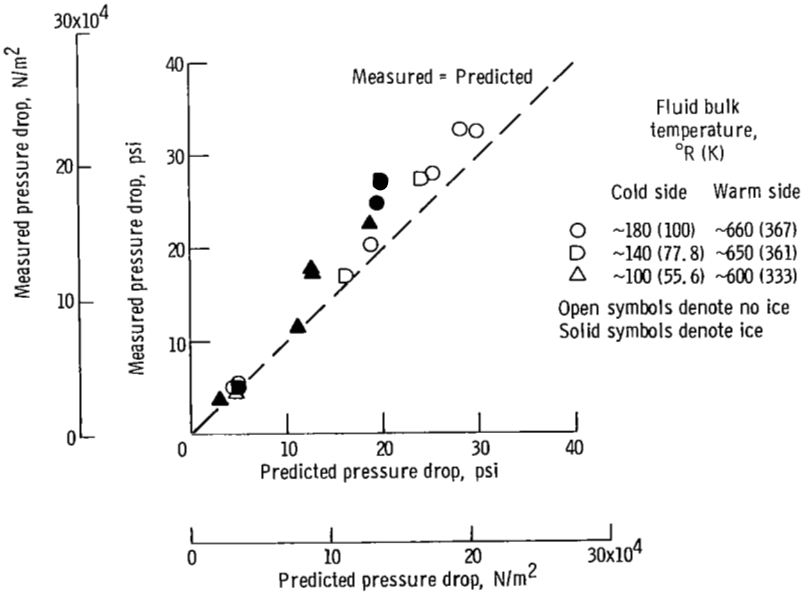

Figure 7. - Comparison of measured to predicted hydrogen pressure drop.

It was shown in the discussion of the overall heat-transfer coefficient that the agreement between the experimental and predicted overall heat-transfer coefficient is improved by increasing the water-side coefficient by 20 percent. The effect on the predicted hydrogen pressure drop as a result of this increase in the fluid heat-transfer coefficient is small. The pressure drop in the non-ice region increases by approximately 2 percent and in the ice region by 4 to 9 percent. Thus the agreement between the measured and predicted pressure drop is slightly improved.

Pressure Drop - Water Side

The water-side pressure drop was measured across a 2-foot (60.9-cm) straight section centered between the water inlet and outlet. The measured pressure drop for isothermal conditions is shown in figure 8 as a function of water flow rate. A dashed curve is drawn through the data. Included for comparison is a curve representing the pressure drop predicted for a smooth passage.

The measured pressure drop is approximately three times that of a smooth passage.

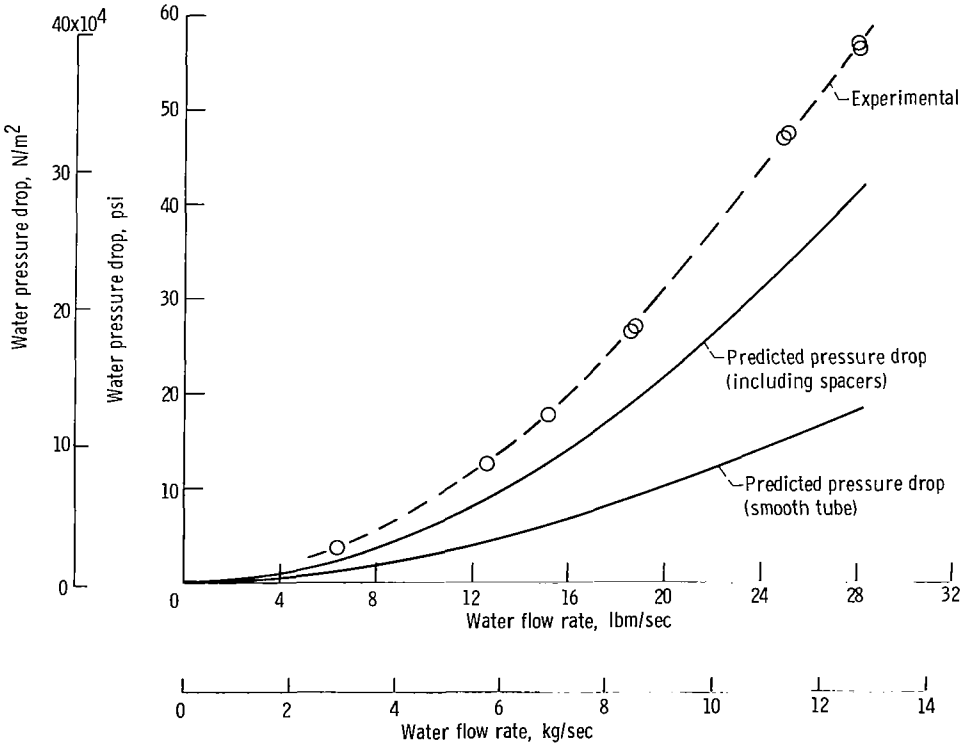

Figure 8. - Isothermal water pressure drop for center 2 feet (0.609 m) of heat exchanger. Fluid bulk temperature, 534° R (297 K).

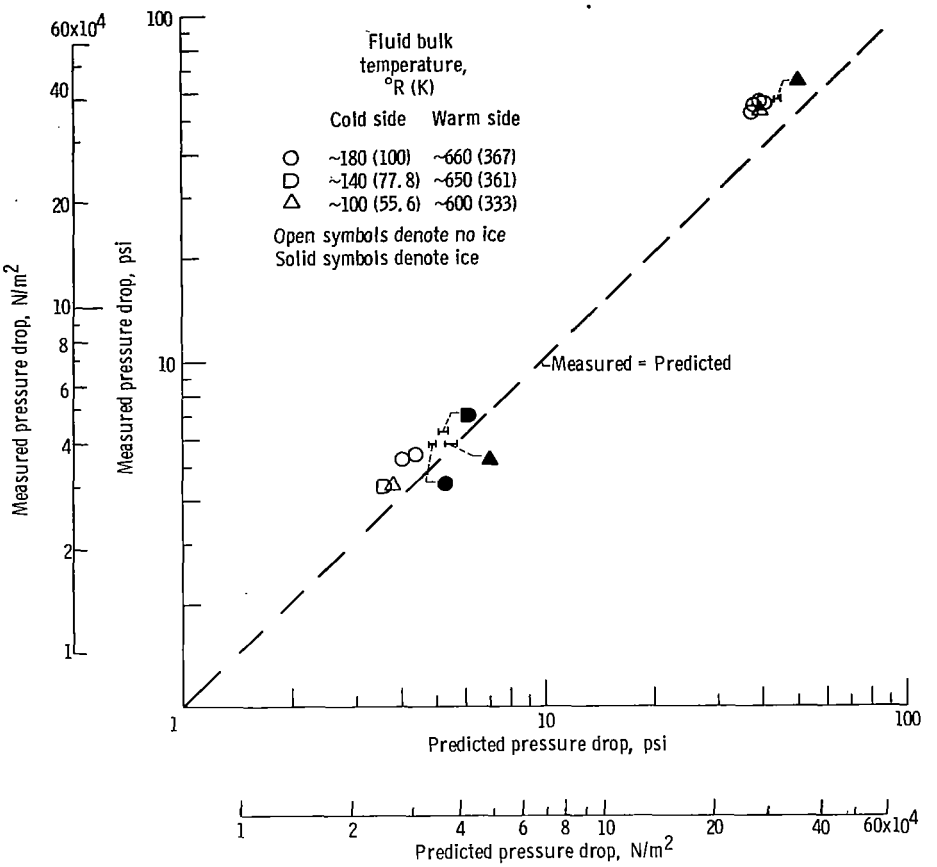

Figure 9. - Comparison of experimental to predicted water pressure drop.

This large difference indicates that some consideration must be given to the pressure loss across the tube spacers.

Spacers were located at six stations between the pressure taps. Spacers at three of the stations resulted in a reduction in flow area of 30 percent, and spacers at the other three stations a reduction of 17 percent. The pressure loss across the spacers at each location was calculated assuming sudden contraction and expansion. The sum of these losses was added to the pressure loss predicted for a smooth passage and the results are shown in figure 8. As a result of including the spacers, the difference between measured and predicted pressure drop was reduced to approximately 40 percent.

In figure 9 the measured pressure drop with heat transfer is compared with the predicted value. As was done with the predicted overall heat-transfer coefficient, a pressure drop was calculated for two water-side heat-transfer coefficients. One assumes a water-side coefficient for a smooth passage, and the second assumes a 20-percent increase in the coefficient. When no ice is predicted (open symbols) the effect of this variation in the water-side heat-transfer coefficient is negligible and the predicted pressure

drop is represented by a single value. In the ice region (solid symbol), the pressure drop decreases with increasing water-side heat-transfer coefficient because of decreased ice blockage of the water passage. The corresponding change in the predicted pressure drop is represented by a horizontal line drawn through each data point. The lowest value is that calculated assuming a 20-percent increase in the water-side heat-transfer coefficient. This gave the best agreement between ice and non-ice data. The predicted pressure drop includes that due to the spacers.

It can be seen in figure 9 that the measured pressure drop with heat transfer, as for isothermal conditions, is greater than predicted. When no ice is predicted, the data range from 16 to 40 percent above the predicted value.

Since the measured pressure drop with and without heat transfer is significantly greater than predicted for a smooth passage, it is reasonable to expect that the water-side heat-transfer coefficient will also be greater than predicted for a smooth passage. An increase in the water-side coefficient did improve the agreement between the measured and predicted overall heat-transfer coefficient as well as improving the agreement between the ice and non-ice fluid pressure drop data. Therefore, the added turbulence apparently resulting from the tube spacers warrants some increase in the water-side heat-transfer coefficient.

Transient Conditions

During startup of the reactor, the heat exchanger would be operating under transient conditions. During the first part of the startup, only a small amount of heat will be added to the water as the gamma heating rate will be small and the structural members of the reactor will be thermally cool. Therefore, care will have to be taken in programing the hydrogen and water flow rates to avoid freezing to the point of blockage of the water passage. Since heat transfer under transient conditions is not well understood, tests were conducted to gain some insight into the characteristics of the heat exchanger under transient conditions.

The transient conditions of interest were those that might occur during reactor startup. To simulate these conditions the hydrogen and water inlet temperature, inlet pressure, and flow rate were programed to vary with time in such a way as might occur during startup. One such ramp is shown in figure 10 when the inlet temperatures and flow rates are shown as a function of time. The inlet pressures vary linearly with time and are tabulated for time equal zero and 30 seconds (end of ramps). This ramp represents an increase from 17 percent of full power to full power in 30 seconds. Each data point represents the average of 24 readings taken over a period of 0.6 second. Prior to the start of the transient, an attempt is made to obtain steady-state conditions for the

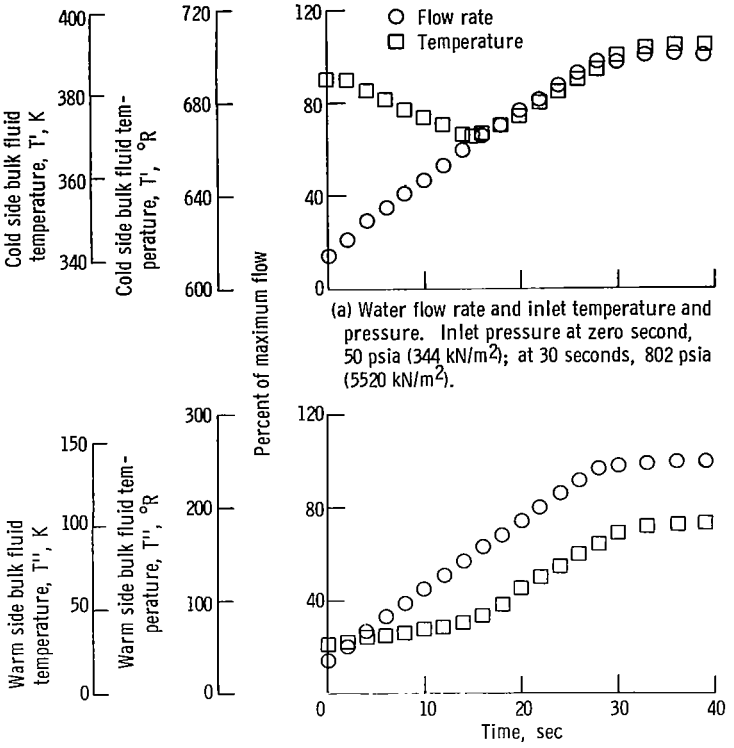

(a) Water flow rate and inlet temperature and pressure. Inlet pressure at zero second, 50 psia (344 kN/m^2); at 30 seconds, 802 psia (5520 kN/m^2).

(b) Hydrogen flow rate and inlet temperature and pressure. Inlet pressure at 0 second, 87 psia (606 kN/m^2); at 30 seconds, 733 psia (5050 kN/m^2).

Figure 10. - Ramped parameters as function of time for 30-second transient.

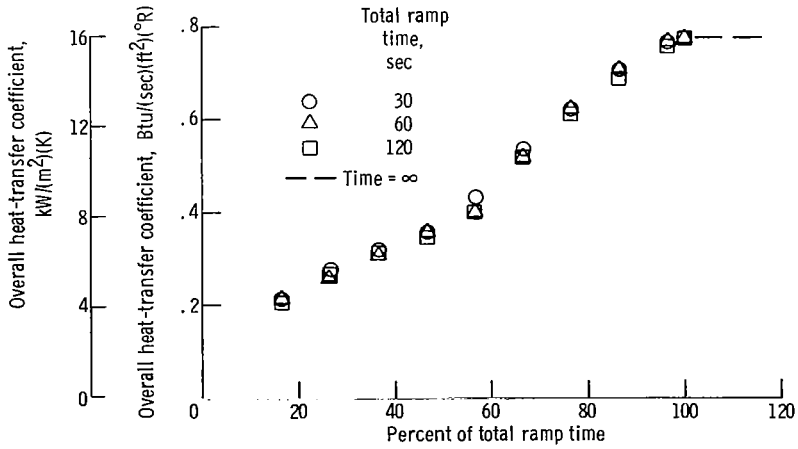

Figure 11. - Comparison of overall heat-transfer coefficient at various ramp rates.

conditions at time equal zero. Steady-state conditions are never quite realized as it is difficult to control the flow rate of the various fluids at these low flows.

The overall heat-transfer coefficients obtained from the run shown in figure 10 are plotted as a percentage of the total ramp time in figure 11. Included for comparison are two runs that have total ramp times of 60 and 120 seconds. The value of the ramped parameters are the same as those in figure 10 when determined on the basis of percentage of total ramp time. Therefore, the ramp rate of the 60-second run is 1/2 that of the 30-second ramp, and the 120-second ramp rate is 1/4. Values below 16 percent of total ramp time are not included because the hydrogen pressure and/or temperature were near the critical value and hence the value of the inlet enthalpy was uncertain.

Examination of the figure shows no detectable effect of ramp rate on the transient overall heat-transfer coefficient. It can also be seen that the heat-transfer coefficient at the end of the ramp (100 percent ramp time) is in good agreement with the value measured at steady-state conditions.

A comparison of the heat-transfer coefficient for transient conditions to the measured steady-state value is shown in figure 12. Here the heat-transfer coefficients are plotted for a 30-second ramp similar to the one shown in figure 10 but with a water inlet temperature 40° R (22.2 K) lower. Included for comparison are three steady-state values, one at 26 percent, one at 60 percent, and one at 100 percent of total ramp time. There is good agreement between steady-state and transient values at 26 and 100 percent of total ramp time, but at 60 percent the transient value is 12 percent below the measured steady-state heat-transfer coefficient. The disagreement at 60 percent of total ramp time may be the result of a hydrogen inlet temperature that was lower in the transient than steady-state run. As was shown in the steady-state section of the investigation the heat-transfer coefficient decreases with decreasing hydrogen inlet temperature.

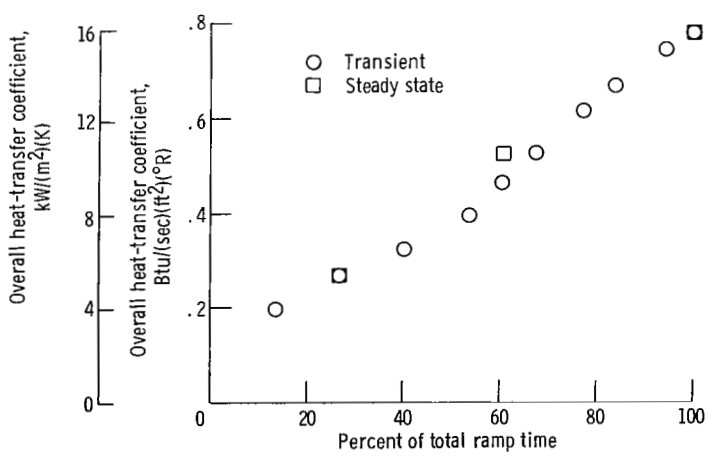

Figure 12. - Comparison of steady-state and transient overall heat-transfer coefficient.

It appears from examination of figures 11 and 12 that the ramp rates investigated are low enough that for this heat exchanger the transient overall heat-transfer coefficient can be reasonably well represented by the steady-state values.

SUMMARY OF RESULTS

The overall heat-transfer coefficient and fluid pressure drops were measured and compared with predicted values for a shell-and-tube heat exchanger. The heat exchanger investigated is of a design that would be suitable for regeneratively cooling the water in a water-moderated nuclear rocket reactor.

The heat exchanger consists of 19 tubes arranged in triangular array within the shell. The fluid was in parallel flow with cryogenic hydrogen in the tubes and water in the shell.

The range of conditions investigated included steady-state and transient operation. For steady-state operation the range of conditions were inlet hydrogen temperature, 100° to 180° R (55.6 to 100 K); inlet water temperature, 600° to 660° R (333 to 367 K); inlet fluid pressures of approximately 700 psia (483×10^4 N/m^2); and fluid flow in the turbulent range. The transient conditions investigated included those that might be expected during startup of the nuclear reactor.

The results of the investigation can be summarized as follows:

Steady-state conditions:

1. Steady-state operation of the heat exchanger was attained at fluid conditions where ice was predicted.

2. The overall heat-transfer coefficient increases with increasing hydrogen flow rate until ice is formed. Once ice is formed the overall coefficient remains essentially constant with increasing hydrogen flow rate.

3. The experimental overall heat-transfer coefficient is in good agreement (approx. ±10 percent) with the predicted value at conditions where no ice is predicted. Where ice is predicted the measured value is 15 to 35 percent above the predicted heat-transfer coefficient.

4. The measured hydrogen side pressure drop is within 20 percent of the predicted value at conditions where no ice is predicted. Where ice is predicted the measured pressure drop generally exceeds the predicted value by more than 20 percent.

5. The measured water-side pressure drop for isothermal conditions is approximately three times greater than predicted for flow in a smooth passage. The measured pressure drop is about 40 percent greater than predicted if pressure loss due to sudden contraction and expansion at each tube spacer is included.

6. The water-side pressure drop with heat transfer and where no ice is predicted exceeds the predicted value by 16 to 40 percent. The measured pressure drop in the ice region is somewhat below the non-ice data.

7. An increase in the predicted water-side heat-transfer coefficient will improve the agreement of the measured and predicted overall heat-transfer coefficient in the predicted ice region. The agreement between pressure drop measurements in the ice and non-ice regions will also be improved by an increase in the water-side heat-transfer coefficient.

Transient conditions:

8. Over the range of ramp rates investigated the overall heat-transfer coefficient can be reasonably well represented by the steady-state value at corresponding fluid conditions.

Lewis Research Center,
National Aeronautics and Space Administration,
Cleveland, Ohio, June 24, 1969,
120-27-04-54-22.

APPENDIX A

SYMBOLS

A	cross sectional flow area
c_p	specific heat at constant pressure
c_v	specific heat at constant volume
D	tube inside diameter
D_e	equivalent diameter of flow passage
D_i	diameter at interface between water and solid surface
D_o	tube outside diameter
f	friction factor
G	mass velocity, w/A
g	acceleration due to gravity
H	enthalpy
h	fluid film heat-transfer coefficient
J	heat of conversion
K	ice thermal conductivity
K_m	metal tube thermal conductivity
k	fluid thermal conductivity
L	total heat-transfer length of heat exchanger
l	incremental length
N	number of tubes
P	wetted perimeter of flow passage
Pr	Prandtl number, $c_p\mu/k$
p	static pressure
Δp	static pressure drop
Δp_{fr}	frictional pressure drop
Δp_{mom}	pressure drop due to change in momentum
Q	heat transferred
Q_L	heat lost
R	gas constant
Re	Reynolds number, GD_e/μ
S	heat-transfer surface area
T	fluid bulk temperature
T_b	average fluid bulk temperature
T_f	fluid film temperature
T_i	interface temperature between water and solid surface
ΔT_m	log mean temperature difference
T_w	wall temperature
t	static temperature
U	overall heat-transfer coefficient
V	velocity
w	mass flow rate
x	distance from heat exchanger inlet to midpoint of increment
γ	ratio of specific heats, c_p/c_v
μ	viscosity of fluid
ρ	density of fluid
ρ_{ave}	average density of fluid

Subscripts:

b bulk (when applied to fluid properties, indicates evaluation at average bulk temperature)

f film (when applied to fluid properties, indicates evaluation at film temperature)

w wall (when applied to fluid properties, indicates evaluation at wall temperature)

1 inlet

2 outlet

Superscripts:

' warm fluid side (water)

'' cold fluid side (hydrogen)

APPENDIX B

MATHEMATICAL ANALYSIS

The analytical program was used to determine the characteristics of a shell-and-tube heat exchanger that utilizes a coolant at a temperature below the freezing point of the liquid being cooled. Here, the parameters of interest are the overall heat-transfer coefficient, the heat flux, the frozen layer thickness, the temperature change of the fluids, and the pressure drop.

For no heat loss to the surroundings and no axial heat conducted along the tubes or shell, the heat given up by the water is equal to that absorbed by the hydrogen and is represented by the equation

$$Q = w''c_p''(T_2'' - T_1'') = w'c_p'(T_1' - T_2') \tag{B1}$$

The equations of heat transfer between the fluids are

$$Q = h'\pi D_i \ell N(T_b' - T_i) \qquad \text{water film} \tag{B2}$$

$$Q = K \frac{2\pi\ell N}{\ln \frac{D_i}{D_o}} (T_i - T_w') \qquad \text{ice layer} \tag{B3}$$

$$Q = K_m \frac{2\pi\ell N}{\ln \frac{D_o}{D}} (T_w' - T_w'') \qquad \text{wall} \tag{B4}$$

$$Q = h''\pi D\ell N(T_w'' - T_b'') \qquad \text{hydrogen film} \tag{B5}$$

The average coolant temperature T_b'' and liquid temperature T_b' are defined as

$$T_b'' = \frac{T_2'' + T_1''}{2} \tag{B6}$$

$$T_b' = \frac{T_2' + T_1'}{2} \tag{B7}$$

The water-ice interface temperature T_i is defined as

$$T_i = T'_w$$

when $T'_w > 492^\circ$ R (273 K)

$$T_i = 492^\circ \text{ R}$$

when $T'_w \leq 492^\circ$ R (273 K). When $T'_w > 492^\circ$ R (273 K), $D_i = D_o$, and no ice is present.

The heat-transfer coefficients are calculated from the following equations.

Hydrogen side from reference 4:

$$h'' = 0.021\left(\frac{k''}{D''_e}\right)_b (Re'')_b^{0.8} (Pr'')_b^{0.4} \left(\frac{T''_w}{T'_b}\right)^{-(0.29+0.0019\, x/D''_e)} \tag{B8}$$

where the properties are evaluated at the gas bulk temperature for the increment l and x is the distance from the inlet of the heat exchanger to the midpoint of the increment. The fluid properties of hydrogen were obtained from reference 3.

Water side from reference 5:

$$h' = 0.034 \frac{k'_f}{D'_e}\left(\frac{\rho'_f V'_b D'_e}{\mu'_f}\right)^{0.8} (Pr'_f)^{0.4} \left(\frac{L}{D'_e}\right)^{-0.1} \tag{B9}$$

A constant L/D'_e of 120 was assumed. Equation (B9) was obtained for air which has a Prandtl number of approximately 0.7. The Prandtl number for water ranges from 2 to 12 for the temperatures of interest herein. Numerous equations similar to equation (B9), some of which include a range of Prandtl numbers, can be found in the literature. One such equation (from ref. 6) for a Prandtl number range of 0.7 to 120 is

$$h = 0.023 \frac{k_b}{D_e} Re_b^{0.8} Pr_b^{1/3} \left(\frac{\mu_b}{\mu_w}\right)^{0.14}$$

The heat-transfer coefficient for water calculated using this equation is within approximately 5 percent of that using equation (B9) over the range of temperatures investigated herein. This is within the accuracy expected for either equation. Thus, although equation (B9) was used for this investigation, either equation would give approximately the same results. The fluid properties in equation (B9) are evaluated at the film temperature defined as

$$T_f = \frac{T_i + T'_b}{2} \tag{B10}$$

The properties of water were obtained from references 7 and 8.

The outlet fluid temperature and hence the heat flux and frozen layer thickness can be calculated from equations (B1) to (B10) for known values of inlet temperatures and mass flow rates. Since the heat-transfer coefficient and ice layer thickness are not constant over the entire length of the heat exchanger, the heat exchanger was divided into small increments over which the heat-transfer coefficient and the ice layer thickness could be considered constant. Calculations could then be performed for each increment starting at the exchanger inlet where the fluid temperatures are known.

Solving equations (B1) to (B10) involves iteration for each increment which results in numerous calculations. For this reason the problem was programed for use on a high speed digital computer. The procedure used for solving the case of parallel flow is described in the following paragraphs.

The tube is divided into increments of length l, and a heat balance is written on the increment assuming that

(1) No heat is lost to the surroundings.

(2) No heat is conducted axially.

(3) At any axial cross section conditions are similar for all tubes.

(4) Temperature and velocity profiles are fully developed.

The known parameters are w', w'', D, D_o, L, number of tubes, and inside diameter of the shell. The equivalent diameters D'_e and D''_e are calculated from the equation

$$D_e = \frac{4A}{P} \tag{B11}$$

The calculations begin with the first increment at the exchanger inlet where T'_1 and T''_1 are known. A value is assigned to the temperature rise of the hydrogen for an increment. This temperature rise must be small so that the heat-transfer coefficients remain nearly constant. The values of T'_2, T''_2, T'_b, and T''_b are then solved for using equations (B1), (B6), and (B7).

The remainder of the equations are solved using an iterative process. The fluid heat-transfer coefficients are solved for using equations (B8), (B9), and (B10), by assuming no ice and making an initial guess at the values of T'_w, T''_w, and l. The calculated values of the heat-transfer coefficients are then used to solve for T'_w and T''_w in equations (B2), (B4), and (B5) by first solving the equations for Q/l. The new values of T'_w and T''_w are used in equations (B8) to (B10). A solution is reached when the difference between the assumed and calculated values of the wall temperature is less than or equal to $0.001(T'_w - T''_w)$ where $T'_w - T''_w$ is the assumed value. This check is made for both T'_w and T''_w. When the solution is reached (if $T'_w \leq 492^\circ$ R (273 K)), ice is assumed to be present. The calculations for the fluid heat-transfer coefficients and the wall temperatures are repeated to include calculations for the ice layer. In calculating

the water heat-transfer coefficient a new value of D'_e is calculated from an assumed value of D_i. The wall temperatures and D_i are solved for using equations (B2) to (B5). A solution is reached when the difference between the assumed and calculated values of D_i is less than or equal to $0.001(D_i)$ where D_i is the assumed value and the previously described check for T''_w is satisfied.

With T'_w, T''_w, and D_i solved for, the increment l is then solved for using equations (B1) and (B5). Using this value as the assumed l, the process of solving for fluid heat-transfer coefficients, wall temperatures, and D_i is repeated. A solution for increment length l, is reached when the difference between calculated and assumed values is less than or equal to 0.001 foot (0.000304 m). When the solution for l is reached, the heat-transfer calculation can begin on the next increment. Here, T'_1 and T'' are equal to T'_2 and T''_2 of the last increment. The heat-transfer calculations for the entire heat exchanger are completed when the sum of the incremental lengths is within 0.005 foot (0.00153 m) of the total length L. If the sum of the l's is greater than L by more than 0.005 foot (0.00153 m), the temperature rise of the hydrogen for the last increment is reduced. The heat-transfer calculations are then repeated for the last increment to determine l.

The water-side pressure drop is calculated using the equation

$$\Delta p' = \frac{f'(G')^2 \, 2 \frac{l}{D'_e}}{g\rho'_b} \tag{B12}$$

where for $(Re')_f \leq 2500$

$$f' = \frac{16}{(Re')_f} \tag{B13}$$

and for $(Re')_f > 2500$

$$f' = \frac{0.046}{(Re')_f^{0.2}} \tag{B14}$$

The calculations are performed for each increment. The total static pressure drop across the heat exchanger Δp is the sum of the incremental pressure drops.

The pressure drop on the hydrogen side was calculated for each increment from the following equations:

$$\Delta p'' = \Delta p''_{fr} + \Delta p''_{mom} = p''_2 - p''_1 \tag{B15}$$

$$\Delta p''_{mom} = \frac{(G'')^2}{g}\left(\frac{1}{\rho''_2} - \frac{1}{\rho''_1}\right) \tag{B16}$$

$$\Delta p''_{fr} = \frac{f''_f 4\left(\frac{l}{D''_e}\right)\rho''_f (G'')^2}{2g(\rho''_{av})^2} \qquad \text{(ref. 5)} \tag{B17}$$

where

$$f''_f = \frac{16}{Re''_f \frac{\rho''_f}{\rho''_b}} \qquad \text{for } Re''_f \frac{\rho''_f}{\rho''_b} \leq 2500 \tag{B18}$$

$$f''_f = \frac{0.046}{\left(Re''_f \frac{\rho''_f}{\rho''_b}\right)^{0.2}} \qquad \text{for } Re''_f \frac{\rho_f}{\rho_b} > 2500 \tag{B19}$$

A static temperature is required to determine the density of the hydrogen and is calculated from the equation

$$t = T - \frac{V^2}{2g J c_p} = \frac{T}{1 + \frac{\gamma - 1}{2}\left(\frac{G}{p}\sqrt{t + \frac{R}{g\gamma}}\right)^2} \tag{B20}$$

Starting with the first increment where T''_1 and p''_1 are known, the static temperature t''_1 is calculated using equation (B20). Then ρ''_2 is calculated by first assuming $t''_2 = T''_2$ and $p''_1 = p''_2$. Equations (B15) to (B19) are then used to calculate p''_2. The static temperature t''_2 is then calculated using equation (B20). The calculations are repeated using these new values of t''_2 and p''_2. A solution is reached when the calculated static temperature is within 0.5° R (0.28 K) of the assumed value and the calculated static pressure at the outlet is within 0.005 pound force per square foot (34.5 N/m^2) of the assumed value. Calculations are then repeated for the next increment by letting p''_2 and t''_2 of the last increment equal p''_1 and t''_1 of this increment. The total pressure drop for the heat exchanger is the sum of the pressure drop for each increment.

For ease of comparison with experimental results an overall heat-transfer coefficient was calculated from the equation

$$U = \frac{Q}{S'' \Delta T_m}$$

REFERENCES

1. Savino, Joseph M.; and Siegel, Robert: Experimental and Analytical Study of the Transient Solidification of a Warm Liquid Flowing Over a Chilled Flat Plate. NASA TN D-4015, 1967.

2. Williamson, K. D., Jr.; and Bartlit, J. R.: Experimental Study of H_2O-LH_2 and H_2O-LN_2 Heat Exchangers. Advances in Cryogenic Engineering, vol. 10, K. D. Timmerhaus, ed., Plenum Press, 1965, pp. 375-381.

3. Goldberg, Fredric N.; and Haferd, Angela M.: Numerical Procedures for Calculating Real Fluid Properties of Normal and Parahydrogen. NASA TN D-4341, 1968.

4. Miller, John V.; and Taylor, Maynard F.: Improved Method of Predicting Surface Temperatures in Hydrogen-Cooled Nuclear Rocket Reactor at High Surface-to Bulk-Temperature Ratios. NASA TN D-2594, 1965.

5. Humble, Leroy V.; Lowdermilk, Warren H.; and Desmon, Leland G.: Measurements of Average Heat-Transfer and Friction Coefficients for Subsonic Flow of Air in Smooth Tubes at High Surface and Fluid Temperatures. NACA TR 1020, 1951.

6. McAdams, William H.: Heat Transmission. Third ed., McGraw-Hill Book Co., Inc., 1954, p. 219.

7. Hogerton, J. F.; and Grass, R. C., eds.: The Reactor Handbook. Vol. 2. Engineering. USAEC Rep. AECD-3646, May 1955.

8. Keenan, Joseph H.; and Keyes, Frederick G.: Thermodynamic Properties of Steam. John Wiley & Sons, Inc., 1936.

NASA-Langley, 1969 — 33 E-4937